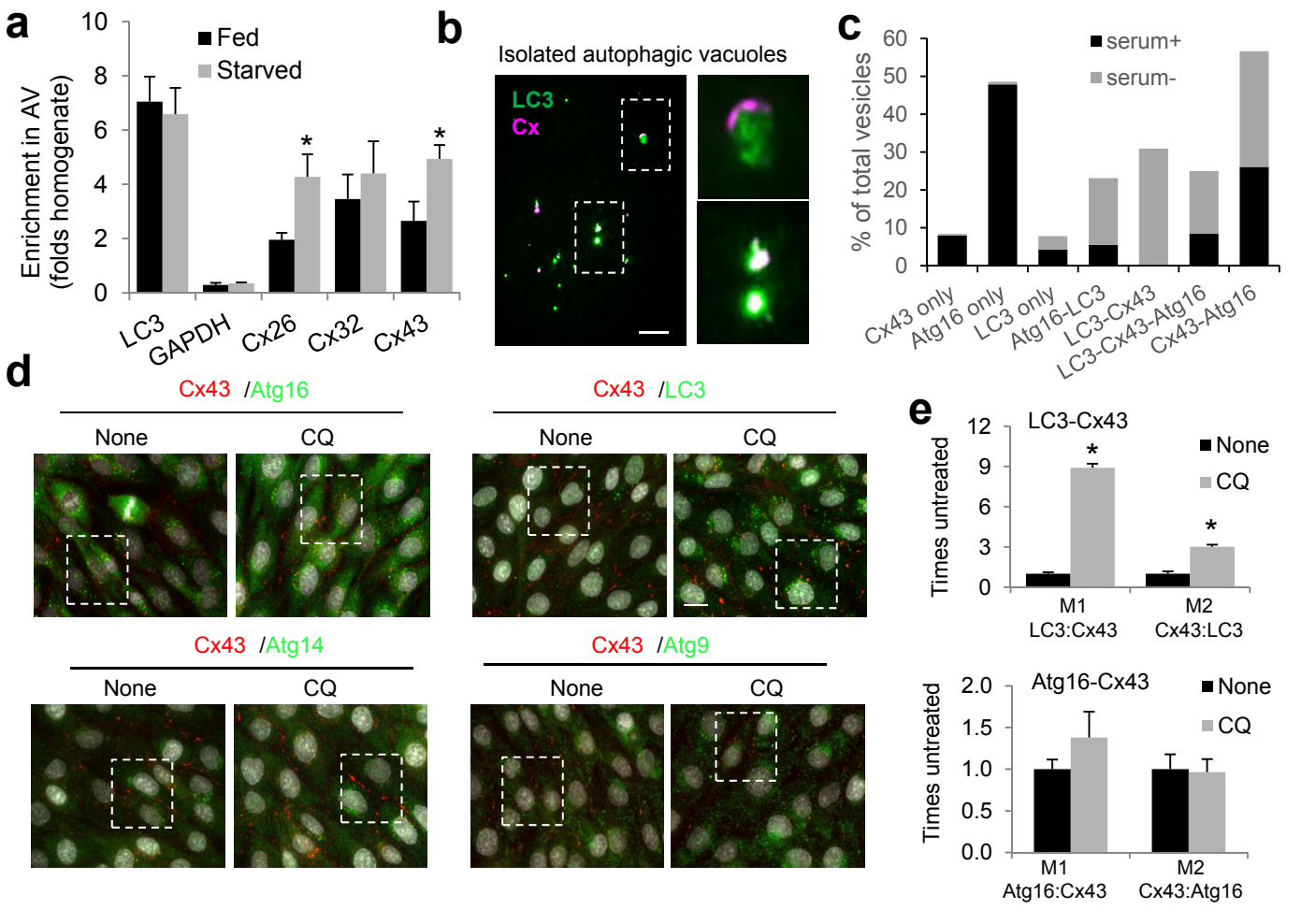

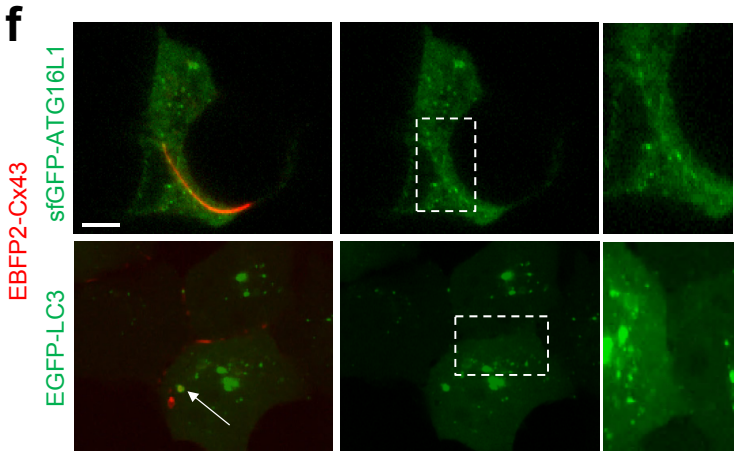

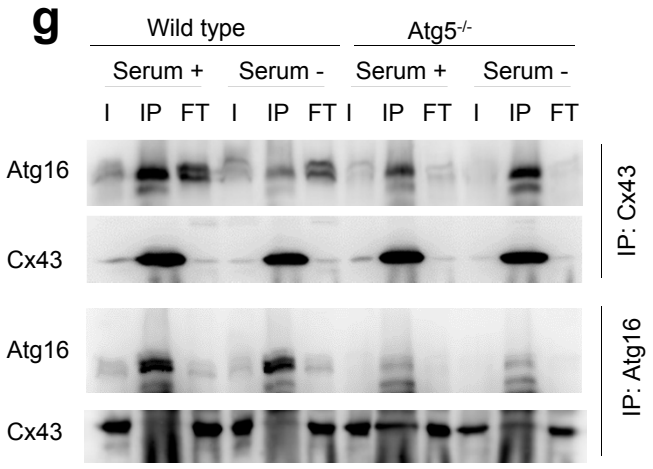

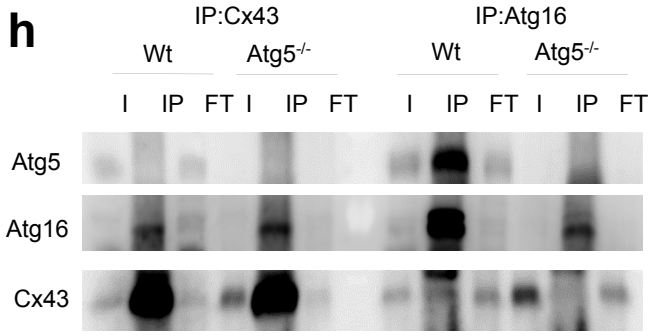

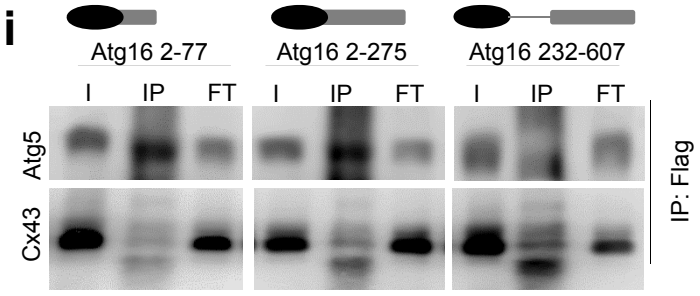

Cuervo - Supplementary Figure 1

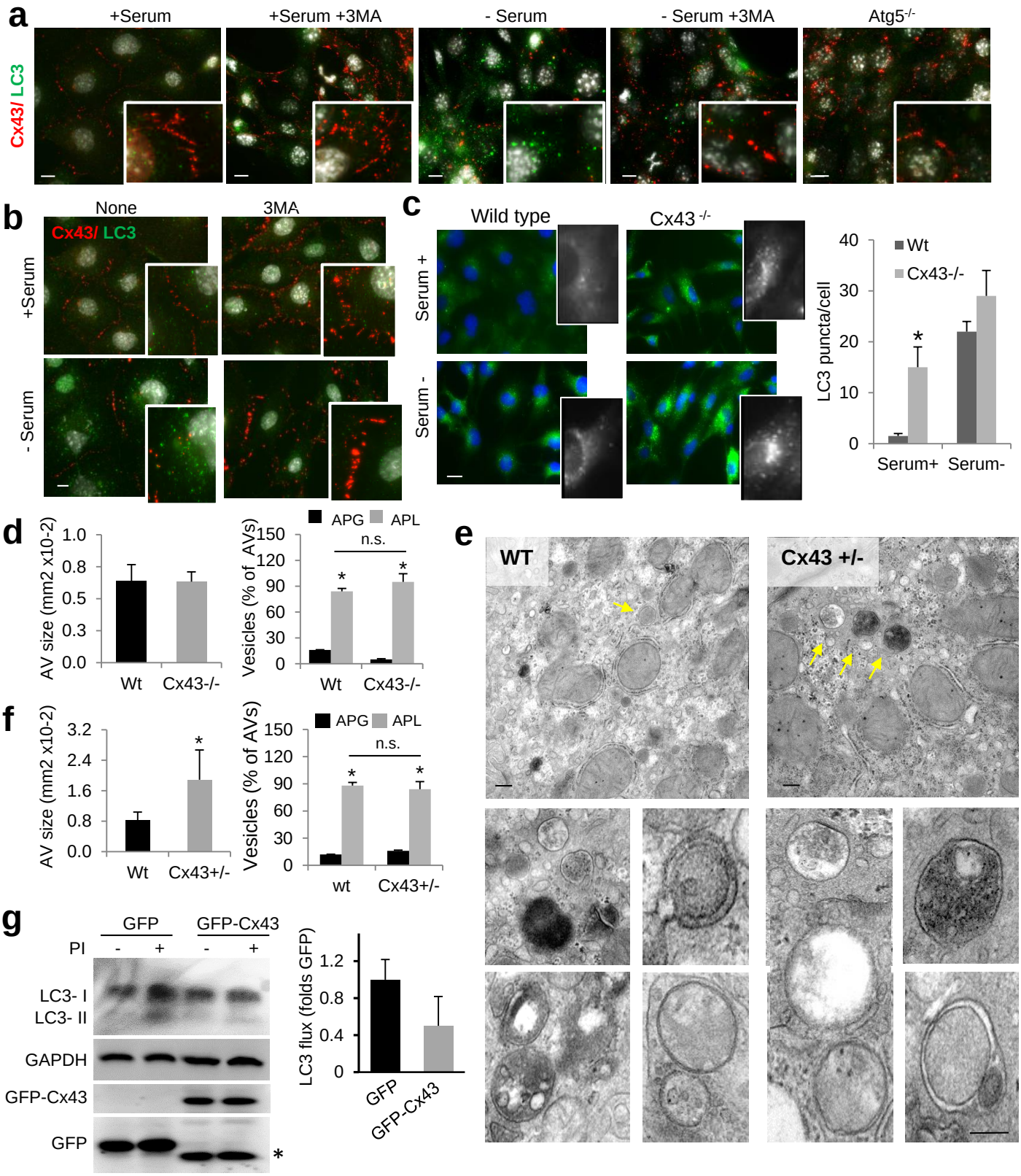

Cuervo - Supplementary Figure 2

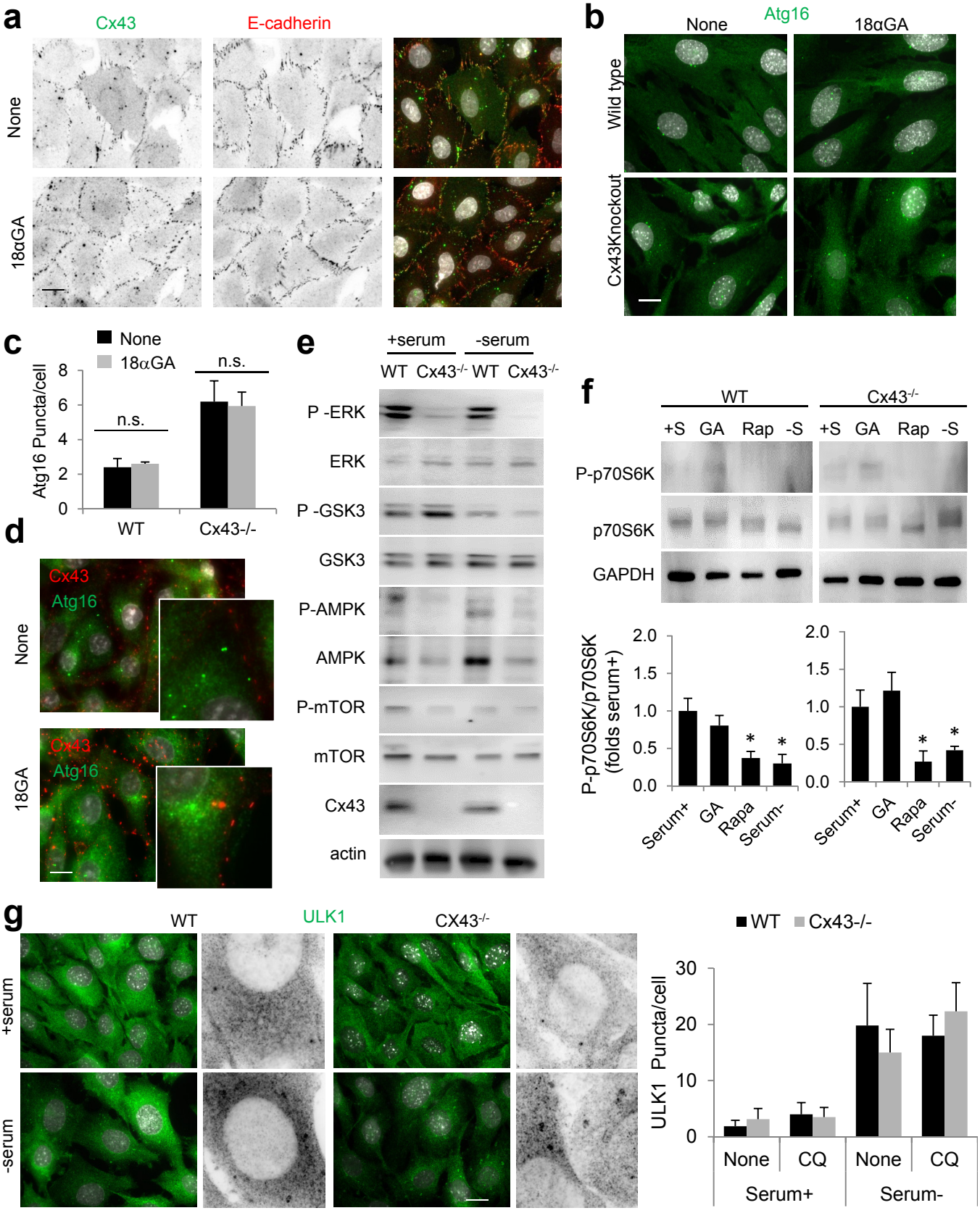
a
Cx43
E-cadherin
None
18αGA
b
None
Atg16
18αGA
Wild type
Cx43Knockout
c
None
18αGA
Atg16 Puncta/cell
n.s.
n.s.
WT
Cx43-/-
d
Cx43
Atg16
None
18GA
e
+serum
-serum
WT Cx43-/- WT Cx43-/-
P -ERK
ERK
P -GSK3
GSK3
P-AMPK
AMPK
P-mTOR
mTOR
Cx43
actin
f
WT
Cx43-/-
+S GA Rap -S +S GA Rap -S
P-p70S6K
p70S6K
GAPDH
P-p70S6K/p70S6K (folds serum+)
Serum+
GA
Rapa
Serum-
g
WT
ULK1
CX43-/-
+serum
-serum
WT
Cx43-/-
ULK1 Puncta/cell
None
CQ
None
CQ
Serum+
Serum-

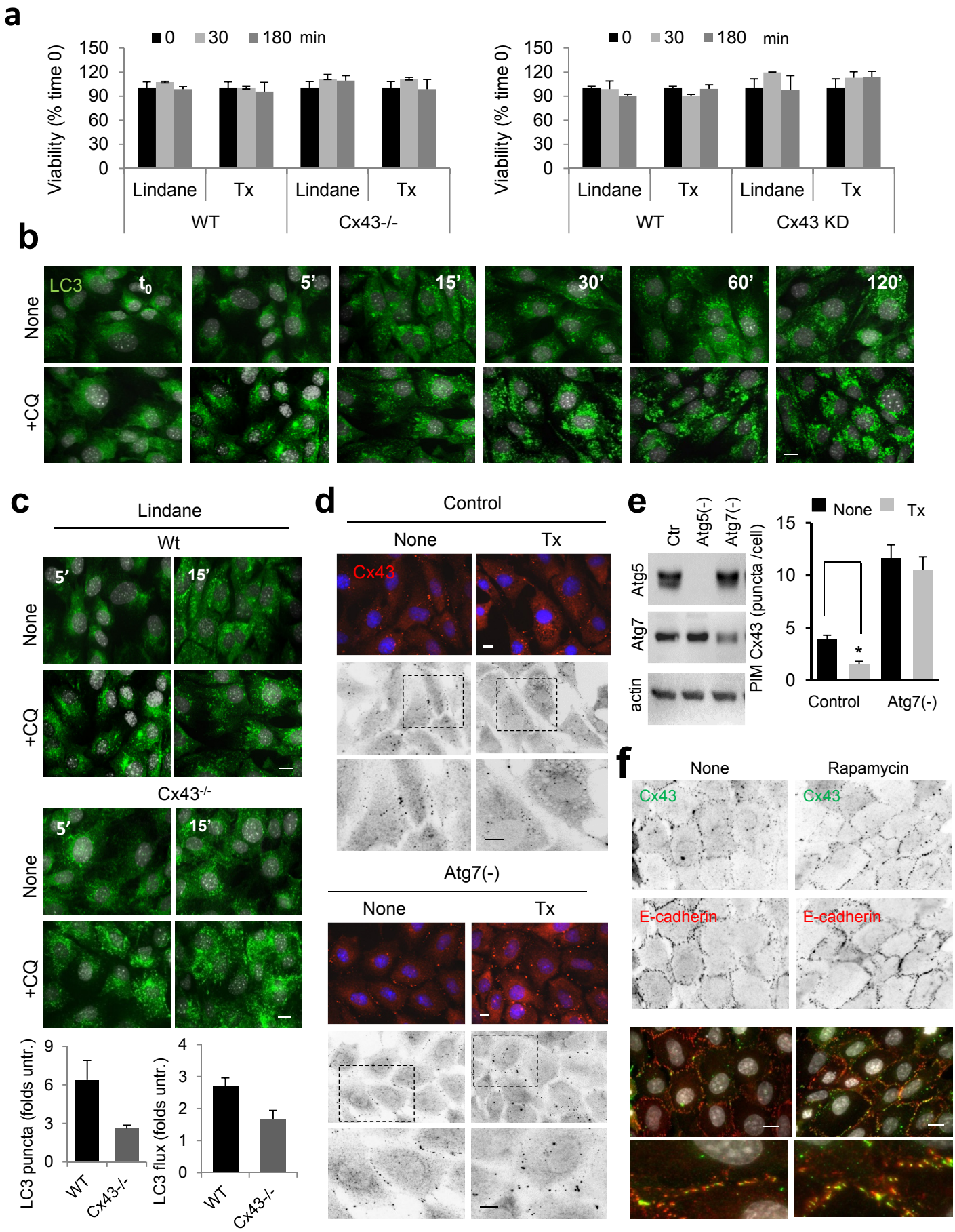

Cuervo - Supplementary Figure 4

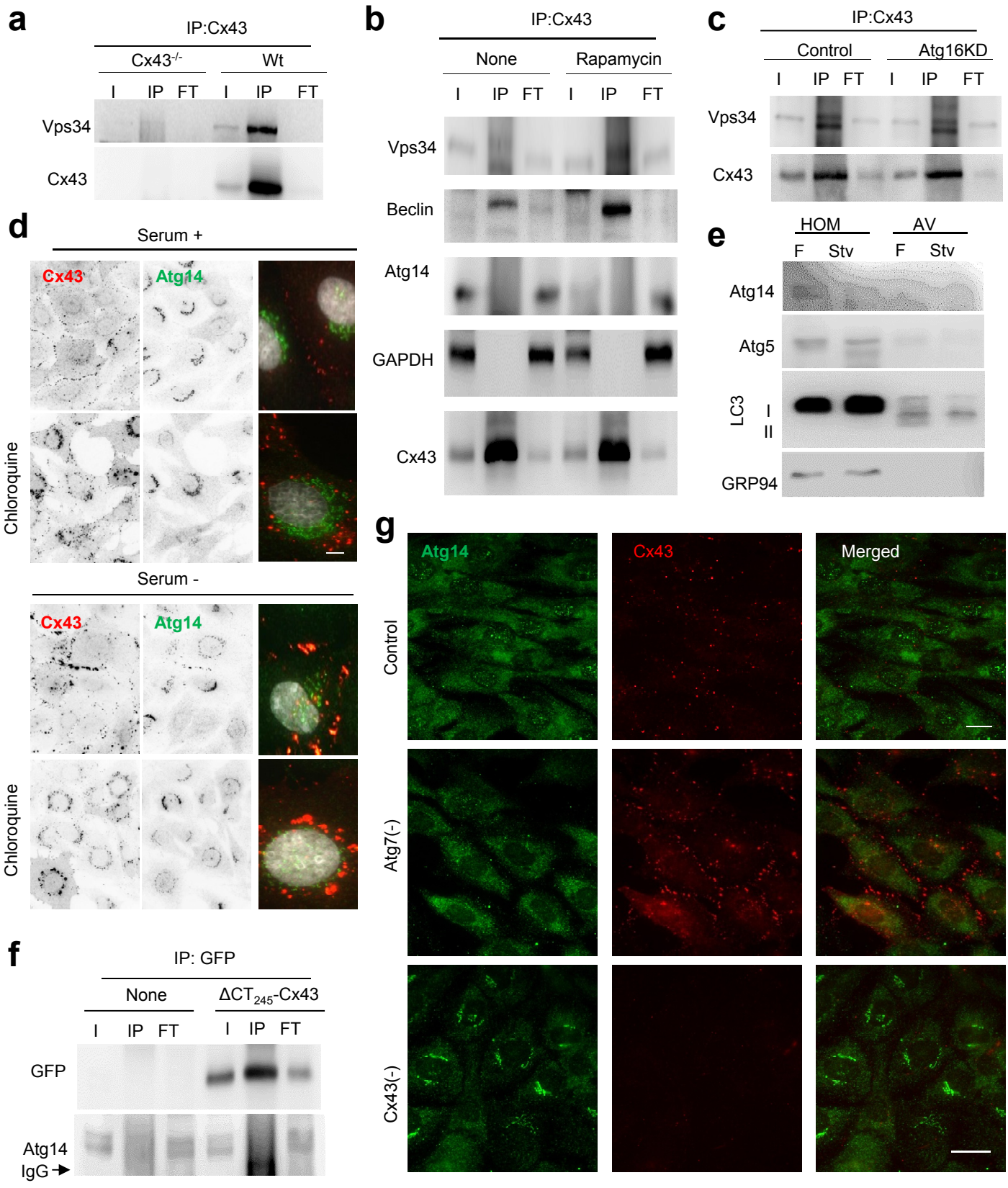

Cuervo.- Supplementary Figure 5

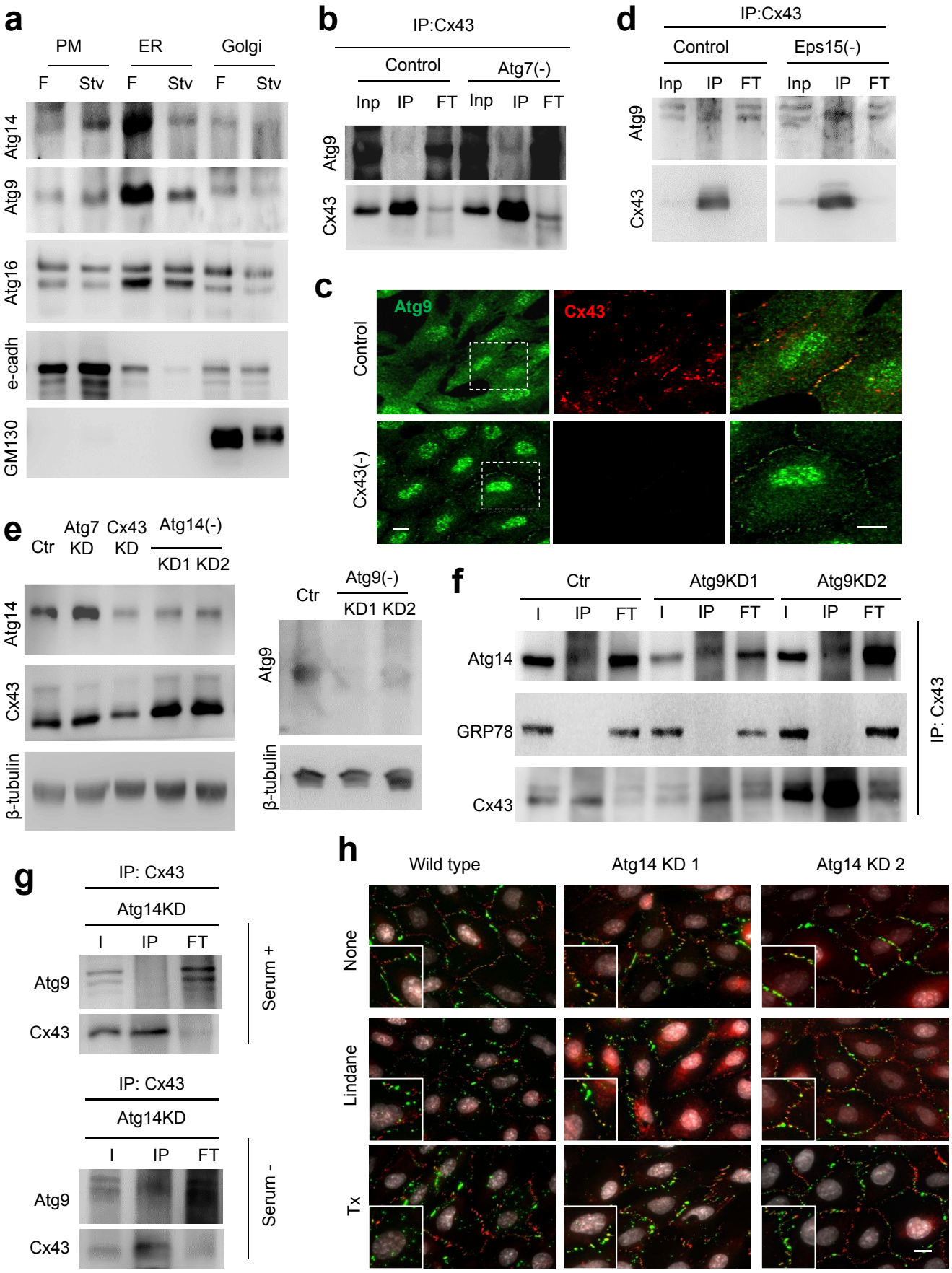

Cuervo - Supplementary Figure 6

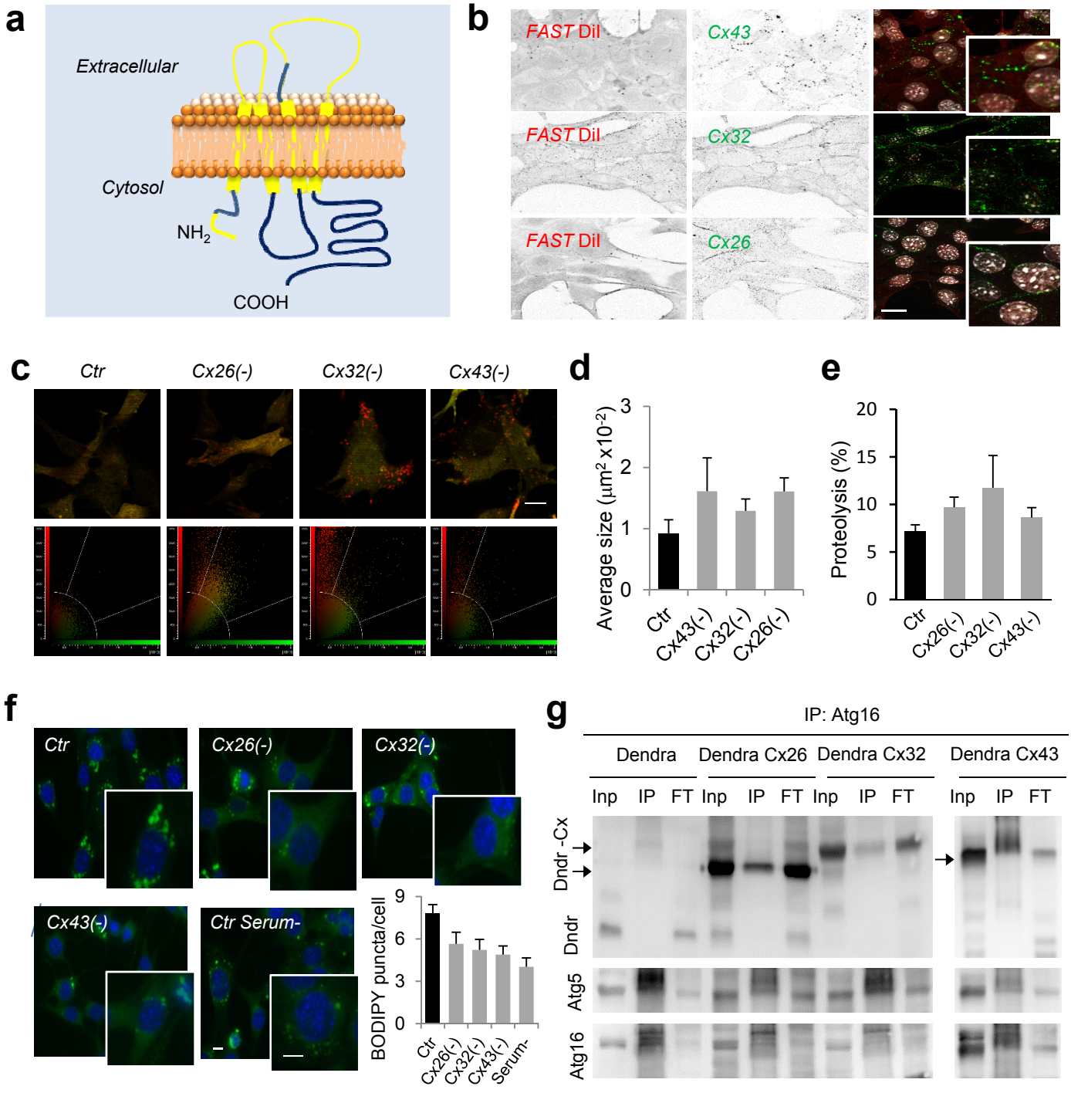

Cuervo - Supplementary Figure 7

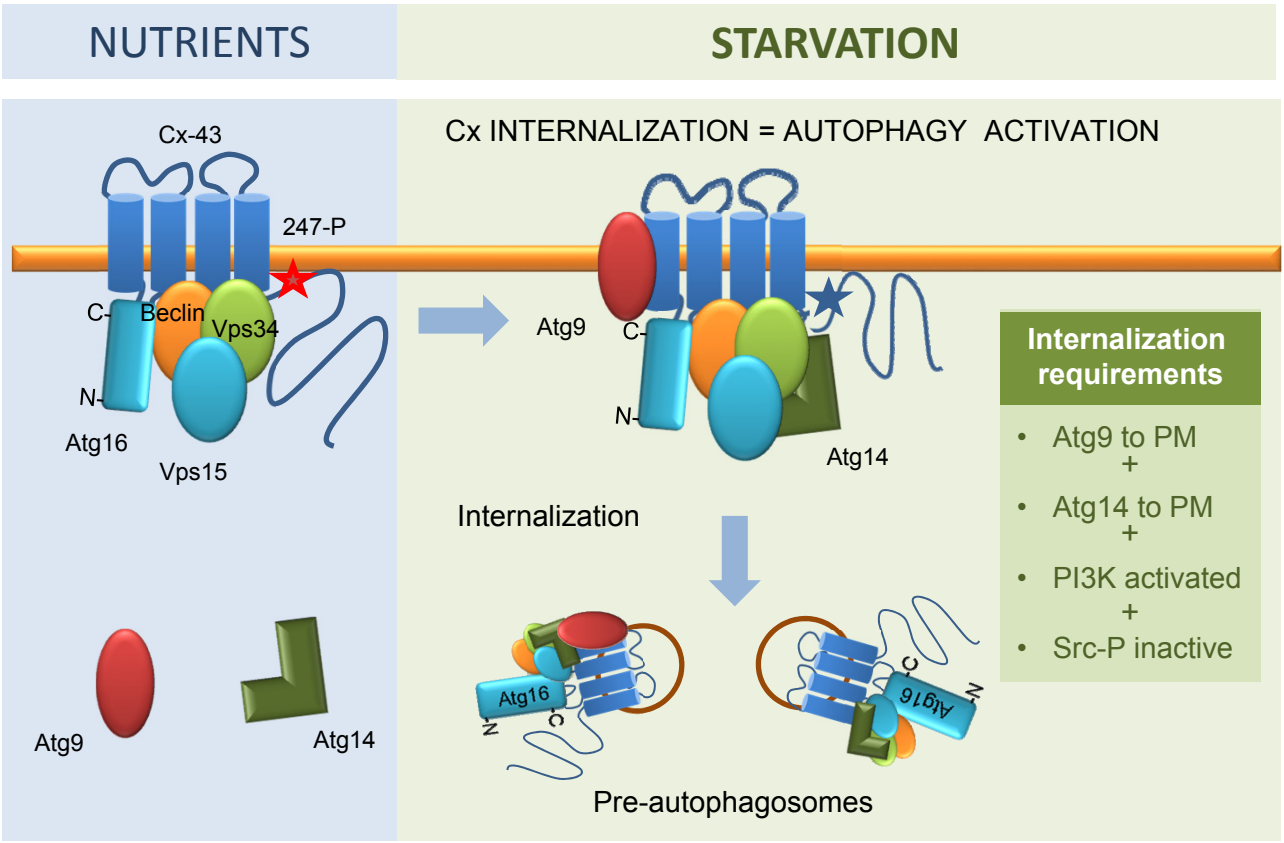

		SERUM-	Cx43 deficient
Cx internalization		Increase	
CX43- BINDING	Cx-PI3K	No change	
	Cx-Atg16	No change	
	Cx-Atg14	Increase	
	Cx-Atg9	Increase	
PLASMA MEMBRANE	PI3K in PM		
	Levels	No changes	Decrease
	Activity	Increase	Decrease
	Atg16 in PM	No changes	Decrease
	Atg14 in PM	Increase	Decrease
	Atg9 in PM	Increase	Increase

Cuervo - Supplementary Figure 8

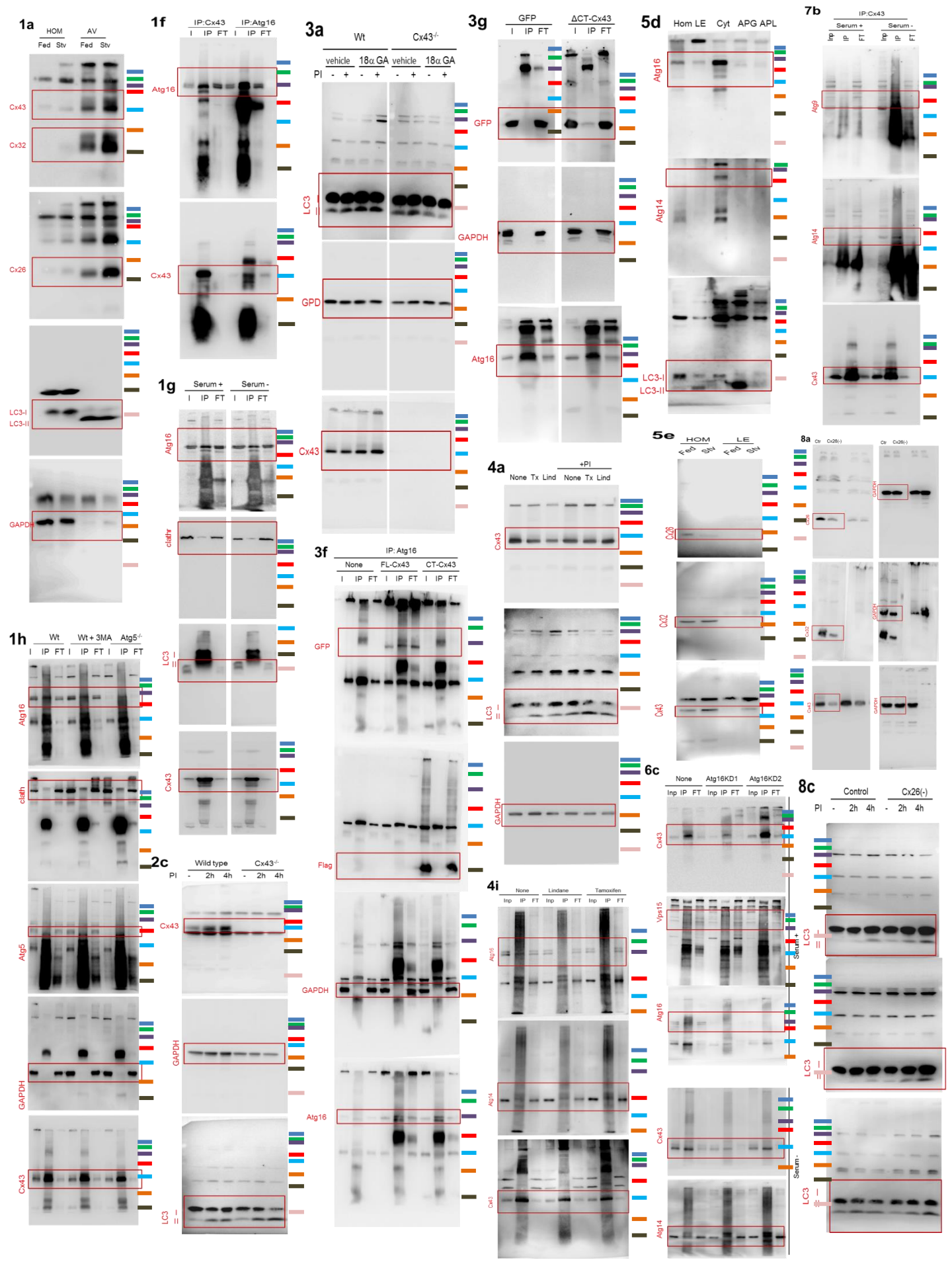
1a
HOM
AV
Fed Stv Fed Stv
Cx43
Cx32
Cx26
LC3-I
LC3-II
GAPDH
1f
IP:Cx43
IP:Atg16
I IP FT I IP FT
Atg16
Cx43
1g
Serum +
Serum -
I IP FT I IP FT
Atg16
clathr
LC3 I II
Cx43
1h
Wt
Wt + 3MA
Atg5-/-
I IP FT I IP FT I IP FT
Atg16
clathr
Atg5
GAPDH
Cx43
2c
Wild type
Cx43-/-
PI - 2h 4h - 2h 4h
Cx43
GAPDH
LC3 I II
Atg16
3a
Wt
Cx43-/-
vehicle
18α GA
vehicle
18α GA
PI - + - + - + - +
LC3 I II
GAPDH
GPD
Cx43
3f
IP: Atg16
None
FL-Cx43
CT-Cx43
I IP FT I IP FT I IP FT
GFP
Flag
GAPDH
Atg16
3g
GFP
ΔCT-Cx43
I IP FT I IP FT
GFP
GAPDH
Atg16
4a
+PI
None Tx Lind None Tx Lind
Cx43
LC3 I II
GAPDH
4i
None
Lindane
Tamoxifen
Inp IP FT Inp IP FT Inp IP FT
Atg16
Atg14
Cx43
5d
Hom LE
Cyt
APG APL
Atg16
Atg14
LC3-I
LC3-II
5e
HOM
LE
Fed Stv Fed Stv
Cx26
Cx32
Cx43
6c
None
Atg16KD1
Atg16KD2
Inp IP FT Inp IP FT Inp IP FT
Cx43
Vps15
Atg16
Serum +
Cx43
Atg14
Serum -
7b
IP:Cx43
Serum +
Serum -
Inp IP FT Inp IP FT
Atg9
Atg14
Cx43
8a
Ctr
Cx26(-)
Ctr
Cx26(-)
GAPDH
Cx26
Cx32
Cx43
8c
Control
Cx26(-)
PI - 2h 4h - 2h 4h
LC3 I II
LC3 I II

Legends to Supplementary Figures

Supplementary Figure 1. Interaction of Cx43 with autophagy compartments at different states of autophagosome formation. (**a**) Enrichment for each of the Cx, LC3 and GAPDH in autophagosomes isolated from fed and starved mice liver. Representative immunoblot is shown in Fig 1a (n=7 blots, 7 mice, 3 different experiments). (**b**) Co-staining for LC3 and Cx43 of isolated autophagic vacuoles spotted on a glass coverslip. High magnification insets are shown in color. (**c**) Percentage of vesicles labeled for each fluorophore in images as the ones shown in Fig. 1b. (n= 3 wells, 3 independent experiments, >20 cells per experiment) (**d**) Immunofluorescence in NRK cells maintained in serum-supplemented media without additions (None) or treated with chloroquine (CQ) for 4h. Boxes are shown at higher magnification in Fig. 1c. (**e**) Colocalization between endogenous Cx43 and different Atg proteins in the same cells shown in d (n= 3 wells, 3 independent experiments and >75 cells or 4 fields). Mander's coefficients are shown as index of colocalization. Colocalization was not detected between Cx43 and Atg14 or Atg9. (**f**) Fluorescence image of HeLa cells expressing EBFP2-Cx43 (pseudocolored in red) and sfGFP-ATG16 (top) or EGFP-LC3 (bottom). Merged channels, single green channel and higher magnification of the boxed area are shown. Top left image was used for the 3D reconstruction shown in Fig. 1d. (**g,h**) Immunoblot immunoprecipitates (IP) of Cx43 and Atg16 in mouse embryonic fibroblasts (MEFs) from wild type (Wt) and Atg5 knock-out mice ($Atg5^{-/-}$) maintained in the presence (g,h) or absence of serum (h). I: input; FT: flow through. (**i**) Immunoblot for Atg5 and Cx43 of immunoprecipitates for flag in Wt MEFs transfected with the indicated flag-tagged constructs of truncated Atg16. All values are expressed as mean+s.e.m. and differences with untreated cells were significant for (*) $p<0.01$. Bars: 1μm panel b and 10 μm rest of panels.

Supplementary Figure 2. Cells deficient in Cx43 have upregulated autophagy. (**a,b**) Immunofluorescence for Cx43 and LC3 in MEFs (**a**) and NRK cells (**b**) maintained in the presence or absence of serum and treated or not with 3-methyladenine (3MA). MEFs from Atg5 null mice are shown in **a** as negative control. Insets: higher magnification. Nuclei were highlighted with DAPI. (**c**) Immunofluorescence for LC3 in mouse osteoblasts (MOB) isolated from wild type (Wt) or Cx43 null mice ($Cx43^{-/-}$) maintained in the presence or absence of serum. Right: Average number of LC3

puncta per cell (n=3 wells, 3 independent experiments, >75 cells per experiment). (**d**) Morphometric analysis of electron micrographs of Wt and Cx43$^{-/-}$ MOB maintained in the presence of serum as the ones shown in Fig. 1b. Values show the average size (left) and the percentage of total autophagic vacuoles (AV) that are autophagolysosomes (right) (n= 3 wells, 3 independent experiments, >10 micrographs). (**e**) Electron micrographs of livers from Wt and Cx43$^{+/-}$ mice. *Bottom:* Representative images of autophagosomes and autophagolysosomes. (**f**) Morphometric analysis of micrographs as the ones shown here to show the average size (left) and the percentage of total autophagic vacuoles (AV) that are autophagolysosomes (right) (n= 3 mice, 3 independent experiments, 10 micrographs per mice). (**g**) Immunoblot for LC3 in MEFs cells transfected with GFP or GFP-Cx43 and treated with proteinase inhibitors (PI) for two hours. (*) non relevant band. Right: LC3 flux relative to the one in GFP transfected cells (n=5 blots, 5 independent experiments). Immunoblots of expression of recombinant proteins are shown. All values are mean+s.e.m. and differences with control were significant for (*) $p<0.01$. Bars: 10 μm.

Supplementary Figure 3. The inhibitory effect of Cx43 on autophagy is independent from other Cx-related cellular functions. (**a**) Co-staining for e-cadherin and Cx43 in NRK treated (or not) with 18αGA. (**b,c**) Representative pictures of staining for Atg16 in mouse osteoblasts (MOB) isolated from wild type (Wt) or Cx43 null mice (Cx43$^{-/-}$) maintained in the presence or absence of 18αGA (**b**) and quantification of Atg16-positive puncta per cell (**c**) (n=3 wells, 3 independent experiments, >30 cells per experiment). (**d**) Co-staining for endogenous Cx43 and Atg16 in untreated (top) or 18αGA-treated (bottom) NRK cells. (**e**) Representative immunoblots for different signaling pathways effectors in Wt or Cx43$^{-/-}$ MOBs maintained in the presence or absence of serum. (**f**) Representative immunoblots for phospho- and total-p70s6k in Wt or Cx43$^{-/-}$ MOBS treated as indicated (top) and quantification of immunoblots as the ones shown (bottom) (n=3 blots, 3 independent experiments). (**g**) Immunostaining for ULK1 in Wt or Cx43$^{-/-}$ MOBs maintained in the presence/ absence of serum and treated or not with chloroquine for 4h. Representative pictures of untreated cells (left) and quantification of ULK1-positive puncta (right) are shown (n=3 wells, 3 independent experiments, >30 cells per experiment). All values are mean+s.e.m. and differences with control were significant for (*) $p<0.01$. Bars: 10 μm.

Supplementary Figure 4. Effect of tamoxifen and lindane on connexin internalization and autophagy. (**a**) Cell viability assay in Wt or Cx43$^{-/-}$ MOB (left) and NRK control or knockdown for Cx43 (right) treated with tamoxifen (Tx) or lindane for indicated times. (n=6 wells, 3 independent experiments) (**b**) Representative images of the time course of

changes in LC3-positive puncta per cell after addition of lindane to control MOB and supplementation or not with chloroquine (CQ) shown in Fig. 4c. (**c**) LC3 immunostaining of MOB from wild type (Wt) or Cx43 knock-out mice ($Cx43^{-/-}$) at the indicated times after lindane addition. *Bottom:* quantification of the folds change in the amount of LC3 puncta per cell (left) and LC3-II flux (right) when compared with untreated cells (n=3 wells, 3 independent experiments, >30 cells per experiment). (**d**) Immunofluorescence for Cx43 in NRK cells control or knocked down (-) for Atg7 untreated or upon addition of Tx. Color images (nuclei are stained with DAPI) and inverted black and white images are shown. Boxed areas are shown at higher magnification (**e**) Immunoblot for the indicated proteins in cells knocked-down for Atg5 and Atg7 and amount of Cx43 remaining in the plasma membrane in control and knock-down cells for Atg7 untreated or treated with Tx (data from panel d). (n=3 wells, 3 independent experiments, >30 cells per experiment). (**f**) Co-staining for e-cadherin/Cx43 in NRK cells treated (or not) with rapamycin for 4 hours. All values are mean+s.e.m. and differences with control were significant for (*) $p<0.01$. Bars: 10 μm

Supplementary Figure 5. PI3K complex associates to the PM in a Cx43-dependent manner. (**a**) Immunoblot for the indicated proteins of immunoprecipitates (IP) of Cx43 in mouse osteoblasts (MOBs) from mice wild type (Wt) or knock-out for Cx43 ($^{-/-}$) maintained in the presence of serum. I: input; FT: flow through. (**b**) Immunoblot for the indicated proteins of Cx43 IP in mouse embryonic fibroblasts (MEFs) treated or not with rapamycin for 4 hours. (**c**) Immunoblot for the indicated proteins of Cx43 IP in MEFs from Wt or knockdown for Atg16 maintained in the presence of serum. (**d**) Co-staining for Atg14 and Cx43 in NRK cells maintained in the presence or absence of serum and treated or not with chloroquine for 4h. Inverted black and white single channel images and inset of merged channels (color) at high magnification. Untreated panels are the wide fields from where inserts shown in Fig 6e were obtained. (**e**) Immunoblot for the indicated proteins of homogenates (HOM) and autophagic vacuoles (AV) isolated from fed and 6h starved (Stv) mice. (**f**) Immunoblot for the indicated proteins of GFP IP in $Cx43^{-/-}$ MEFs control (None) or expressing $\Delta CT_{245}Cx43$ and maintained in serum supplemented media. (**g**) Immunostaining for Atg14 and Cx43 in NRK cells control or knocked down (-) for the indicated proteins. Single and merged channels are shown. Higher magnification of the boxed area is shown. Bars: 10 μm.

Supplementary Figure 6. Dynamic interaction of Cx43 with pre-autophagosomal components. (a) Immunoblot for the indicated proteins in subcellular fractions from liver of fed (F) or 6h starved (Stv) rats. PM: plasma membrane; ER:

endoplasmic reticulum. (**b**) Immunoblot for Atg9 in immunoprecipitates (IP) of Cx43 in NRK cells control and knocked down for Atg7 maintained in the absence of serum. (**c**) Immunostaining for Atg9 and Cx43 in NRK cells control and knocked down for Cx43. Single and merged channels at higher magnification of the boxed areas are shown. (**d**) Immunoblot for Atg9 in immunoprecipitates (IP) of endogenous Cx43 from control and Eps15 knockdown NRK cells. I: input; FT: flow through. (**e**) Immunoblot for the indicated proteins of NRK cells control (Ctr) or knocked-down (-) as labeled. Two different shRNA (sh) against Atg14 (left) and against Atg9 (right) are shown. (**f**) Immunoblot for Atg14 in Cx43 IP from control and Atg9(-) NRK cells maintained in serum-free medium for 4 hours. (**g**) Immunoblot for Atg9 in Cx43 IP from control and Atg14(-)NRK cells maintained in presence or absence of serum for 4 hours. (**h**) Representative pictures for the immunofluorescence for e-cadherin and Cx43 in NRK cells control or Atg14(-) maintained in the presence or absence of tamoxifen (Tx) or lindane. Quantification and higher magnification insets in Fig 7h. Bars: 10 μm.

Supplementary Figure 7. Changes in autophagy in mouse embryonic fibroblasts (MEFs) knocked down for different connexins. (**a**) Scheme of Cx at the plasma membrane. The highly conserved part of their sequence is highlighted in yellow, whereas divergent regions are shown in blue. (**b**) Representative pictures of immunofluorescence for Cx (green) in MEFs stained with the *FAST* Dil (a dye which diffuses laterally within PM) (red) (**c**) Images of cells control (Ctr) or knocked-down (-) for the indicated Cx transfected with the mCherry-GFP-LC3 tandem reporter. Three representative images and representative cytofluorograms are shown. (**d**) Average area of the autophagic vacuoles detected in MEFs Ctr or (-) for the indicated connexins. (n=3 wells, 3 independent experiments, >10 micrographs per well). Representative images are shown in Fig. 8e. (**e**) Long half-life protein degradation in the same cells as in c. Values are shown as the percentage of proteolysis (n=3 wells, 3 different experiments, triplicate aliquots). (**f**) BODIPY 493/503 staining of the same cells loaded with 0.06mM oleic acid for 24h and incubated for 12h in serum-supplemented or serum-free medium, as labeled. Right: Quantification of the average number of BODIPY puncta per cell (n=3 wells, 3 independent experiments, >30 cells per well). (**g**) Immunoblot for the indicated proteins of Atg16 immunoprecipitates in MEFs transfected with the vectors coding for the fluorescent protein Dendra or Dendra fused to Cx26, Cx32 and Cx43. The blot on the right is of lower percentage to resolve Cx43 better.Atg5 is shown as positive control of Atg16 interaction. All values are mean+s.e.m. ANOVA+Bonferroni test was applied to experiments in panels d, e and f, but differences were not statistically significant. Bars: 10 μm

Supplementary Figure 8. Hypothetical model of the inhibitory effect of plasma membrane Cx on autophagosome biogenesis. Under basal conditions (left) Cx43 sequester autophagy initiators and autophagosome precursor at the plasma membrane. During starvation (right) the coincident arrival of Atg14 and Atg9 to the plasma membrane and the resulting activation of Vps34 kinase activity induce internalization of the Cx-Atg complex and the delivery of these pre-autophagosome components to sites of autophagosome formation. Table at the bottom summarizes the changes in the Cx-Atg complex and the association to PM of Atg proteins during nutrient-induced autophagy or in the absence of Cx43.

Supplementary Figure 9. Uncropped images of key panels in main figures. Red boxes indicate the cropped portion of each immunoblot presented in the corresponding main figure. Ladder of molecular weight markers is show on the right of each panel. Color codes are as follows: Blue 130kDa, Green 95kDa, Purple 72 kDa, Red 55 kDa, Cyan 43 kDa, Orange 32 kDa, Grey 26 kDa, Pink 17kDa.